ANNUAL PROGRESS REPORT

TO

THE NATIONAL AERONAUTICS AND SPACE ADMINISTRATION

FOR

NsG 708

A GRANT IN SUPPORT

of

BASIC RESEARCH IN SEMICONDUCTOR DETECTOR-DOSIMETER CHARACTERISTICS, AS APPLIED TO THE PROBLEMS OF WHOLE BODY DOSIMETRY

from

SOUTHERN METHODIST UNIVERSITY
Dallas, Texas 75222

July, 1965

ANNUAL PROGRESS REPORT
NsG 708

I. Experimental Progress

A. Lithium Drifted Silicon Semiconductor Detectors:

1. Fifty different detectors have been incorporated into this study. They represent a family of various sized devices ranging in size from 1 x 1 x 1 mm to 5 x 5 x 130 mm. Long detectors, i.e., having proton path lengths in silicon of 10, 20, 30, 50, 70, 100, 130 and 150 mm are being used to totally absorb high energy protons. Shorter path lengths are used to measure stopping power ($dE/\rho dx$) in silicon.

2. Southern Methodist University now has the capability of fabricating Lithium-drifted detectors of any desired shape. New techniques of fabrication, mounting and encapsulation are being developed.

3. A paper entitled, "Preparation of Lithium Drifted Solid State Detectors" by Bobby D. Snow was presented at the Sixty-eighth annual meeting of the Texas Academy of Science, December, 1964. Abstract in Appendix C.

B. Stopping Power Measurements

1. Data has been taken using protons having energies of 5, 6, 8, 10, 11, 12, 13, 14, 15, 16, 36, 37, 40, and 187 Mev. Absorbers were used in duplicate sets of three different thicknesses permitting measurements on six different absorbers with each of two or more detectors.

   a. Metals: Aℓ, Cu, Si, C.
   b. Plastics: Nylon, plexiglass, polyethylene.
   c. Tissue: Bone, muscle, fat.

2. A paper entitled, "Stopping Power Measurements of Aℓ., Cu., and Si. Using 36.1 Mev Protons" by Daniel C. Nipper was presented at the Sixty-eighth annual meeting of the Texas Academy of Science, December, 1964. Abstract in Appendix C.

3. Appendix B is a description of the data analysis procedure.

C. Charge-pulse response of silicon detectors

1. The charge-pulse response of many of the detectors have been measured for the proton energies listed in B as a function of proton energy, proton path length in silicon and operating conditions of the detector. The average energy required to produce an ion-electron pair has been obtained from both the stopping power measurements in silicon and from the protons totally absorbed in silicon.

These data are required to translate the current from each detector produced by a known radiation flux density and stored in a calibrated condenser into doses, i.e., the total energy absorbed per unit mass of silicon.

2. A paper entitled, "Experimental Calibration of Lithium Drifted Silicon Detectors as a Function of Proton Energy and Proton Path Length in the Detector," by George W. Crawford has been accepted for presentation at the September 1965 meeting of the American Physical Society. Abstract in Appendix C.

D. Detector Life-time Behavior Studies:

The depletion depth, volume, noise level, charge pulse per Mev, dark current and capacitance are being measured for each detector used in the study. The complete age-usage history thus obtained over the two-year period will be used to (a) predict the usable life of a detector and (b) to pin-point and predict loss of reliability of data produced by the detector.

E. Field Trips:

1. To the University of Texas, Austin, Texas:

Dates: October 10-11, 1964. Accelerator time: 36 hours. Proton Energies 5-14 Mev.
Dates: December 28-29, 1964. Accelerator time: 36 hours. Proton Energies 8-16 Mev.

2. Oak Ridge National Laboratories, Oak Ridge, Tennessee
Dates: November 21-29, 1964, Accelerator time: 80 hours. Proton Energies: 36-40 Mev.

3. University of Uppsala, Uppsala, Sweden
Dates: October 23-November 8, 1964, Accelerator time: 100 hours, Proton Energy: 187 Mev.

4. University of Southern California, Los Angeles, California
Dates: May 18-22, 1965, Accelerator time: 18 hours. Proton Energies 18-27 Mev.

F. NASA Participation:

Members of the NASA, Manned Space Center, Space Radiation and Fields Branch participated in the research effort at both the University of Uppsala and at Oak Ridge National Laboratory. At each facility additional research of special interest to this Branch were accomplished. These included exposure of nuclear track plate emulsions and calibration of various dosimeters. The accelerator time made available to NASA at no charge ranged from 16 to 24 hours at each facility.

II. Theoretical Progress

A. Linear Stopping Power Calculations:

A program for calculating linear stopping power, $dE/\rho dx$; based on the Bethe-Block equation

$$-\frac{1}{\rho}\frac{dE}{dx} = \frac{Z}{A}M(\beta)\left[\ln\frac{N(\beta)}{I^2} - 2\beta^2 - \delta - \frac{2C(\beta)}{Z}\right]$$

including shell corrections has been completed, tested and used on the SMU, CDC 3400 computer to calculate the correct thicknesses for the pure absorbers, Al, Cu, Si, and C. The mean ionization potential, I, has been evaluated experimentally for each element.

B. Monte Carlo Stopping Power Calculations:

1. The linear stopping power program has been incorporated into a Monte Carlo transport program which permits Coulomb interaction with both the orbital electrons and the nuclei. This program has been used to verify the stopping power measurement and the energy straggle measured experimentally. A description of the program is given in Appendix A.

2. A paper entitled, "Linear and Monte Carlo Calculations of Stopping Power and Energy Straggle" by George W. Crawford was presented at the Sixty-eighth annual meeting of the Texas Academy of Science. December, 1964. Abstract in Appendix C.

C. Determination of Z, A and I for complex absorbers.

The above programs are being used to determine effective Z, A, and I values for water, bone, meat and fat based on the experimental stopping power measurements. The end result will be a program by which dose, i.e., the total energy absorbed per unit mass of the absorbing material, can be calculated as a function of flux density, type and energy of the ionizing radiation.

D. Calculation of Effective Z, A, and I.

1. The effective values of Z, A, and I for each of four plastics studied are being used to obtain a mathematical model for calculating these quantities where the chemical composition and relative abundance of a heterogeneous material is known.

2. A paper entitled, "Preliminary Report of the Experimental Determination of $I_{eff.}$, $Z_{eff.}$, and $A_{eff.}$ in the Bethe-Block Stopping Power Equation for Four Plastics," by James R. Cummins, Jr. was presented at the Sixty-eighth annual meeting of the Texas Academy of Science. December 1964. Abstract in Appendix C.

Annual Progress Report

NsG 708

Appendix B

The extraction of information from proton stopping experiments.

I. Introduction

The object of the experimental study is to assess values of parameters in the Bethe-Block formula that describes the average rate of energy loss suffered by a charged particle along the path of migration in matter in interactions with atomic electrons.

$$-\frac{1}{\rho}\frac{dE}{dS} = \frac{Z}{A} M(\beta)\left[\ln \frac{N(\beta)}{I^2} - 2\beta^2 - \delta - \frac{2C(\beta)}{Z}\right] \qquad (1)$$

where ρ is the density of the medium (in g/cm^3), A is the atomic weight, Z the atomic number, M (β) and N (β) are functions of the velocity $v = \beta c$, I is the mean ionization potential, C (β) is the "shell correction", and δ is the density correction (which is negligible at energies considered here).

The philosophy of the method that is developed for the extraction of information from the experiments is the following: We use the Bethe-Block formula and "reproduce" theoretically the experimental conditions as accurately as possible. We then apply criteria, based on a comparison between experimental and theoretical results to determine the optimum values of the fitting parameters (I and C (β)) and their accuracy, depending on the experimental uncertainties.

The experimental situation is outlined in fig. 1.

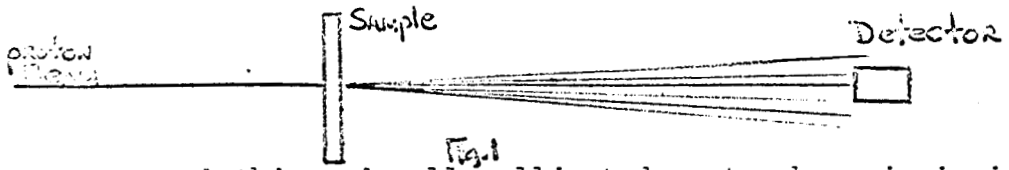

Fig. 1

A thin and well collimated proton beam is incident on a sample of the material under investigation. The lateral extension of the sample is large as compared to the width of the proton beam at every point in the sample. The sample thickness, x, is known to within an accuracy Δx.

The energy spread of the incident proton beam will, at present, be considered small enough for the outcome of the experiment to be unaffected by it. The uncertainty, ΔE_o., in the assessment of the beam energy will, however, be taken into account.

The ideal method for extracting the measured information should include the detector in the "theoretical reproduction" and actually predict the output of the detector. At the present stage of development, our method stops one step short of such an ideal treatment. We make the assumption that the detector is an instrument that measures the energy distribution of the proton number (current) density averaged over the exit surface of the sample. The fact that the detector-sample distance is large is believed to justify this assumption.

The theoretical treatment of the proton transport process is based on a Monte Carlo method described in refs. (1) and (2) but for some minor improvements that will be reported separately.

II. Parametrization of the experimental results.

The measurements result in pulseheight distributions recorded by a multichannel analyzer, i.e. the energy distributions are obtained in a histogram form. It is essential for the following mathematical development that the experimental results be converted into a more suitable, analytical form.

The following ansatz is consistent with the physics of the problem

$$f(x) = \frac{1}{\sqrt{\pi}} \left\{ e^{-t^2} \left[1 + \sum_{r=1}^{N} a_r t^r \right] \right\} \tag{2}$$

$$t = \frac{E - E_a}{\sigma} \tag{2a}$$

in that it represents the measured spectrum to a first-order, gaussian approximation, multiplied by a perturbation function in the form of a polynomial, the parameters of which may be determined from the experimental results. E_a is the average energy in the gaussian approximation and is solved from the equation

$$x = \int_{E_a}^{E_0} \frac{dE}{\left| \frac{dE}{dS} \right|} \qquad [x] = cm \tag{3}$$

where the expression for $\frac{dE}{dS}$ is taken from the Bethe-Block formula with best known values of the parameters. The standard deviation σ is obtained from the approximation formula (ref. 3)

$$\sigma^2 = 2\rho^2 x \qquad [x] = g/cm^2 \tag{4}$$

where

$$\rho^2 = \frac{2C\, m_e c^2 E'_m}{\beta^2}\left(1 - \frac{\beta^2}{2}\right) \qquad (4a)$$

$$2C = 0.30058\,\frac{Z}{A}\ (cm^2/g) \qquad (4b)$$

$$\beta^2 = v^2/c^2$$

$$E'_m = 2 m_e c^2 \frac{p^2c^2}{m_e^2c^4 + m^2c^4 + 2m_e c^2 (p^2c^2 + m^2c^4)^{1/2}} \qquad (4d)$$

m_e is the electron mass.
m " " proton "

and

$$p^2c^2 = \frac{\left[E + mc^2 - \frac{(mc^2)^2}{E+mc^2}\right]^2}{1 - \frac{mc^2}{E+mc^2}} \qquad (4e)$$

An analytical form which is preferable to that of eq. (2) with regard to mathematical convenience and required numerical labor is the following

$$f(x) = \frac{1}{\sqrt{\pi}} \left\{ e^{-x^2} \left[1 + \sum_{r=1}^{N} a_r H_r(x) \right] \right\} \qquad (5)$$

where

$$H_r(x) = (-1)^r e^{+x^2} \frac{\partial^r}{\partial x^r} \left(e^{-x^2} \right) \qquad (6)$$

is the Hermute orthogonal polynomial of order r with normalization

$$\int_{-\infty}^{\infty} e^{-x^2} H_r(x) \, H_\mu(x) \, dx = \delta_{r\mu} \sqrt{\pi} \, 2^r \, r! \qquad (6a)$$

The condition

$$\int_{-\infty}^{\infty} f(x) \, dx = 1 \qquad (7)$$

will always be fulfilled for such a choice of function.

We intend to fit an expression of the form of eq.(5) to the experimental histogram by way of applying a minimum-X^2 criterion to the parameter space $\{a_r\}$. To illustrate our notation we present fig. 2 showing a typical experimental output

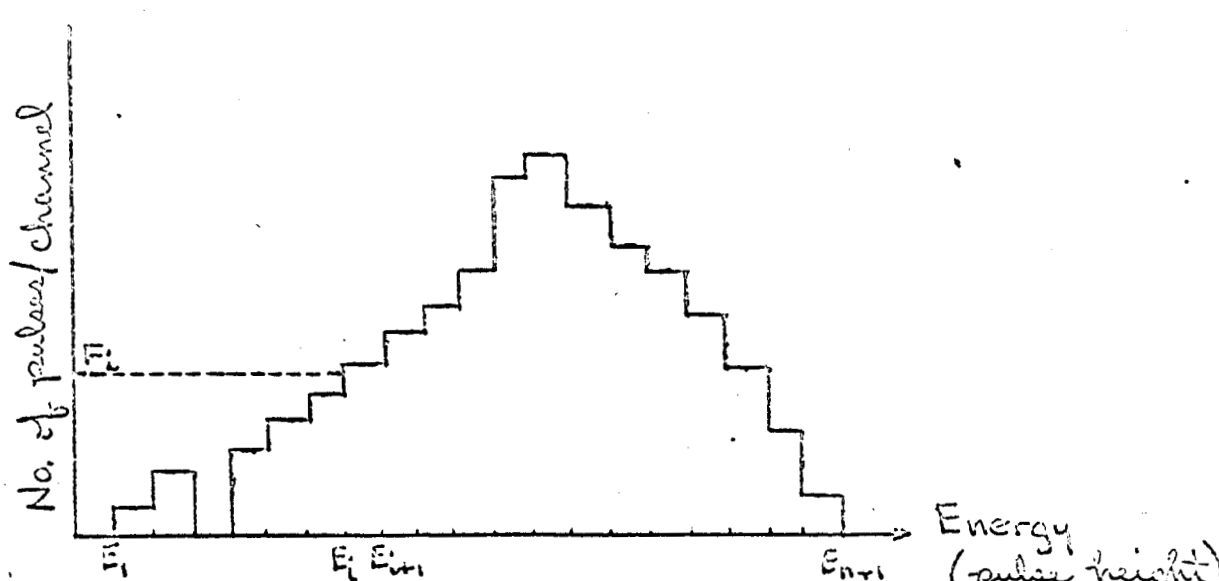

$E_{i+1} - E_i$ = constant = ΔE. (this linearity condition should be scrutinized in the future for possible sources of uncertainty).

F_i = (integral) number of pulses in channel no. i $\left(E_i < E < E_{i+1}\right)$

$$\sum_{i=1}^{n} F_i = F$$

We apply the "modified" minimum-X^2 formalism (ref. 4) according to which the following expression is minimized to produce the optimum values of the a_r.

$$\chi^2 = \sum_{i=1}^{n} \frac{(F_i - \Phi_i)^2}{F_i} \tag{8}$$

where

$$\Phi_i = F \int_{E_i}^{E_{i+1}} f\left[t(E)\right] dt(E) \tag{9}$$

$$t_{i+1} = \frac{E_{i+1} - E_a}{\sigma}$$

$$\Phi_i = F \int \frac{1}{\sqrt{\pi}} \left\{ e^{-t^2} \left[1 + \sum_{r=1}^{N} a_r H_r(t) \right] \right\} dt$$

$$t_i = \frac{E_i - E_a}{\sigma}$$

$$= \frac{F}{\sqrt{\pi}} \left\{ \frac{\sqrt{\pi}}{2} \left(\operatorname{erf} t_{i+1} - \operatorname{erf} t_i \right) + \sum_{r=1}^{N} a_r \left[e^{-t_i^2} H_{r-1}(t_i) - e^{-t_{i+1}^2} H_{r-1}(t_{i+1}) \right] \right\} \tag{9a}$$

using the properties of the Hermite polynomials as given in ref. 5 where the erf functions are also defined.

χ^2, as given in eq. (8), is minimized when

$$\frac{\partial \chi^2}{\partial a_r} = 0 \quad \text{for all } a_r ,$$

i.e.,

$$\sum_{i=1}^{n} \frac{F_i - \Phi_i}{F_i} \times \frac{\partial \Phi_i}{\partial a_r} = 0 \qquad (10)$$

which is a system of N linear equations in $a_1, a_2, \ldots a_r \ldots a_n$.

We must pay attention to the case where Fi assumes the value 0. If this should happen we simply broaden channel i to include also the nearest non-zero channel on the low-Fi side of the empty channel (as well as all the empty channels in between).

The solution of the system (10) is straightforward and results in the assessment of $\{a_r\}$.

We now wish to compute the maximum of the function f(t). Differentiation of eq. (5) gives

$$\frac{d f(t)}{dt} = \frac{1}{\sqrt{\pi}} \left\{ -e^{-t^2} \left[2t + \sum_{r=1}^{N} a_r H_{r+1}(t) \right] \right\} \qquad (11)$$

using again the properties of the Hermite polynomials (refs. 5,6). If the gaussian approximation were correct, the maximum of f(t) would lie at t=0 ($E=E_a$). We may exploit that fact when solving the equation

$$2t + \sum_{r=1}^{N} a_r H_{r+1}(t) = 0 \qquad (12)$$

for that one of its roots, $t = \delta$, which is nearest to t=0.

We have now obtained a value of the most probable energy E_p as determined by the detector.

$$E_p = E_a + \delta\sigma \tag{13}$$

from insertion in eq. (2a).

It is essential that we determine the variance in E_p which results from the stochastic nature of the method employed to measure it. Using statistical theory (ref. 4) we obtain

$$D^2(E_p) = \sum_{r=1}^{N} \left[\frac{\partial E_p(a_r)}{\partial a_r}\right]^2 \times D^2(a_r) \tag{14}$$

where

$$D^2(a_r) = \frac{1}{F\int_{-\infty}^{\infty}\left[\frac{\partial \log f_r(x)}{\partial a_r}\right]^2 f_r(x)\,dx} \tag{15}.$$

Equation (15) may be elaborated on to give

$$D^2(a_r) = \frac{1}{F} \times \frac{1}{\int_{-\infty}^{\infty}\left[\frac{1}{\sqrt{\pi}} e^{-x^2} H_r(x)\right]^2 \times \frac{1}{f_r(x)}\,dx} \tag{15a}.$$

In this context it is justified to set $\frac{1}{f_r(x)} = \sqrt{\pi}\, e^{x^2}$ as a good approximation, giving

$$D^2(a_r) = \frac{1}{F} \times \frac{1}{2^r r!} \tag{16}.$$

We differentiate equation (13) with regard to a_r and obtain

$$\frac{\partial E_p}{\partial a_r} = \sigma \frac{\partial \delta}{\partial a_r} \tag{17}.$$

$\frac{\partial \delta}{\partial a_r}$ may be solved by differentiation of eq. (12) at $t = \delta$:

$$a_r \frac{\partial \delta}{\partial a_r} + H_{r+1}(\delta) + \left[\sum_{r=1}^{N} a_r \frac{\partial H_{r+1}(\delta)}{\partial \delta}\right] \frac{\partial \delta}{\partial a_r} = 0 \tag{18}$$

bearing in mind that δ is a function of all a_r.

Hermite polynomials have the property (ref. 6)

$$2r\,H_{r-1}(x) = \frac{\partial H_r(x)}{\partial x} \tag{19}$$

and therefore

$$\frac{\partial \delta}{\partial a_r} = \frac{-H_{r+1}(\delta)}{2\left\{1 + \sum_{r=1}^{N}\left[(r+1)\,a_r H_r(\delta)\right]\right\}} \tag{20}$$

We have now built up a framework of expressions that permit explicit solution of D (E_p), the standard deviation of the probability distribution of E_p.

At present, we shall let E_p alone symbolize the outcome of a spectrum measurement at one absorber thickness.

The complete spectrum may be written in a more convenient form by shifting the maximum of f(t) to t=0. This is accomplished by setting $E_a \equiv E_p$ in equation (2a) and solving for a new set of $\{a_r\}$. As seen from equation (11) the new a_r will have the property that

$$\sum_{r=1}^{N} a_r H_{r+1}(0) = 0, \text{ i.e.,} \tag{20a}$$

$$\sum_{\substack{r=1 \\ (\text{odd } r)}}^{N} a_r (-1)^{\frac{r+1}{2}} \times \frac{(r+1)!}{\left(\frac{r+1}{2}\right)!} = 0 \tag{20b}$$

III. The detector response function.

As we discussed in the introduction, we consider at present, the origin proton beam to have negligible energy spread with regard to energy variations of the material properties that determine the transport of protons in the medium under consideration. This assumption is not likely to be subject to much dispute. We must, however, also assume that the response characteristics of the detector are such that the maximum of the pulse-height distribution, measured by the detector, coincides with the maximum of the energy distribution of protons transmitted through the sample. As mentioned in the introduction, the later assumption will be removed when the detector will be operationally included in the Monte Carlo transport calculation, used for the "theoretical reproduction" of the experiment. We have provided arguments that point toward the justification of this assumption on a qualitative basis. It is possible, however, to make an a posteriori test of both assumptions, mentioned, in a case where the Bethe-Block parameters are already well established.

Suppose that we have access to a measurement, such as the one shown in fig. 1, but with the absorber removed. We may proceed in the same manner as described in Section II to parametrize the detector output setting E_a equal to the nominal source energy E_o and $\sigma = \sigma_o$ equal to some reasonable value, which may be therated on to produce the most concentrated set of $\{a_r\}$.

Setting $\chi = \frac{E - E_o}{\sigma_o}$

we obtain a source response function $f_o(\chi) = f_o\left(\frac{E - E_o}{\sigma_o}\right)$.

For a reasonably thin sample it may be assumed that the detector response function does not vary its form for energies varying from the source energy to the lowest energy represented by the protons transmitted through the attenuating sample.

Suppose now, that we have obtained a closed expression for the theoretical spectrum of protons escaping through the sample, assuming a discrete source energy E_0. Let us call this distribution function g (E). We perform the folding integral

$$f^*(E) = \int g(E') \times f_0(E - E')\, dE' \qquad (21)$$

to obtain the predicted distribution as measured by the detector with the attenuator thickness at which the theoretical spectrum g (E) was calculated.

A comparison of the position of the maximum of the function $f^*(E)$ with that of the function $f(E) = f_0(E)$, determined in Section II, will provide a test of our assumptions. It is essential that the statistical accuracies be considered in this comparison (cf. eq (14), cf. eq).

We shall look in more detail at the solution procedures for eq. (21).

The function g (E^1) may be written

$$g_0(E') = g(x_1) = \frac{1}{\sqrt{\pi}} \left\{ e^{-x_1^2} \left[1 + \sum_{r=1}^{N_1} b_r H_r(x_1) \right] \right\} \qquad (22)$$

with

$$x_1 = \frac{E' - E_{mc}}{\sigma} \qquad (22a)$$

E_{MC} is the maximum of the Monte Carlo calculated spectrum as obtained from an analysis such as that described in Section II (cf. Section IV). σ is the same dispersion as that obtained from eq. (4). We assume that the maximum of $q_0(E')$ has been made to coincide with that of the limiting gaussian.

The function $f_0(E-E')$ may be written

$$f_0(E-E') = f_0(t_2) = \frac{1}{\sqrt{\pi}}\left\{e^{-t_2^2}\left[1+\sum_{r=1}^{N_2} c_r H_r(t_2)\right]\right\} \qquad (23)$$

$$\text{with } t_2 = \frac{E-E'}{\sigma_0} \qquad (23a)$$

The function $f_0(t_2)$ and its derivation from the source energy response of the detector has been discussed previously in the present section.

Insertion of (22), (22a), (23), (23a) into (21) leads, after some rearrangement, to the expression

$$f^*(E) = \frac{1}{\sqrt{\pi}} \frac{e^{-\frac{(E-E_{MC})^2}{\sigma_0^2+\sigma^2}}}{\sqrt{\sigma_0^2+\sigma^2}} \int_{-\infty}^{\infty} e^{-\left(\frac{k_1 k_2}{\sqrt{1+k_2^2}} - t_1\sqrt{1+k_2^2}\right)^2} \times$$

$$\times \left[1+\sum_{r=1}^{N_1} b_r H_r(t_1)\right]\left[1+\sum_{r=1}^{N_2} c_r H_r(t_2)\right] d\left(\frac{k_1 k_2}{\sqrt{1+k_2^2}} - t_1\sqrt{1+k_2^2}\right) \qquad (2$$

where $k_1 = \frac{E-E_{MC}}{\sigma_0}$ and $k_2 = \frac{\sigma}{\sigma_0}$.

This integral can be performed exactly after another rearrangement and substitution of t_1 and t_2 to the expression in the differential. This is straightforward as t_1, t_2, and the latter expression are all linearly dependent (this is seen by elimination of E^1 between equations (22a) and (23a).

The mathematical labour of treating equation (24) in the way just described has, at the present stage, prevented us from performing this rigorous test analytically. A practical way of doing the same thing in a possibly more illustrative but not so stringent manner is the following: Perform the integration of eq. (21) numerically on a computer and check that the functions $f^{**}(E)$ and f (E) have coinciding maxima. An automatic curve-plotter is very useful for this. This procedure also provides a means for comparing the overall agreement of the experimental and theoretical curves in the case where the parameters of the Bethe-Block equation are known.

IV. Parametrization of Monte Carlo results.

As discussed in the previous section, we assume that the theoretical calculation (using the Monte Carlo procedure of refs. 1 and 2) of the transmitted proton spectrum is available in a closed analytical form. It remains now to determine such an expression from the histogram output of the Monte Carlo calculation. We proceed exactly as in section II. The relation $E_{i+1} - E_i =$ constant is not generally valid in this case, however, but this does not affect the exact applicability of the derivation, as that relation has not been utilized.

We obtain the expression

$$g(x) = g\left(\frac{E - E_{MC}}{\sigma}\right) = \frac{1}{\sqrt{\pi}} e^{-x^2}\left[1 + \sum_{r=1}^{N} \vartheta_r H_r(x)\right] \qquad (22)$$

We also compute the standard deviation $D(E_{MC})$ exactly as we obtained $D(E_p)$ in section II.

V. Determination of parameters in the Bethe-Block equation.

The principle that we want to apply when deriving the resulting optimum values of the mean ionization potential I and the shell correction function C is the following: Compare the measured and calculated values of the most probable energy of transmitted protons (E_p and E_{MC}, respectively) and form the deviation

$$\Delta E_p = E_p - E_{MC} \tag{25}$$

We then want to use this quantity to determine what values of our "unknown" parameters would have made $\Delta E_p = 0$. assuming ΔE_p to be small we would then use the best available values of $\frac{dE_p}{dI}$ and $\frac{dE_p}{dC}$ to obtain the necessary adjustments in the known parameters. I is a constant but C is a function of energy, and therefore, we need measurements at many energies to determine C(E). An iterative procedure, in which the new values of I and C were used to recalculate the derivatives $\frac{dE_p}{dI}$ and $\frac{dE_p}{dC}$, as well as the theoretical maximum E_{MC} will lead to a final determination of optimum parameter values. We shall, however, as already once before, stop at a lower degree of sophistication at the present stage of development.

We may use the calculations of Sternbeimer (ref. 7) of the quantity

$$q(E) = \frac{I}{R} \times \frac{dR}{dI} \tag{26}$$

which is the fractional change of R for a given small fractional change of I. R is the proton range from the source energy to 2 MeV. in Sternbeimer's approximation the shell (and density) corrections are considered to be functions of I only.

We shall assume in this approximation, that the protons suffer no angular deviations and that the simple continuous slowing down approximation is valid. We may then use Sternbeimer's tables of q vs. E for various materials. We shall discuss the details of this procedure.

$$\text{Set } q_o = q(E_o) = \frac{I}{R_o} \times \frac{dR_o}{dI} \tag{27}$$

where R_o is the range from the source energy to 2 MeV. Analogously,

$$q_p = q(E_p) = \frac{I}{R_p} \times \frac{dR_p}{dI} \tag{28}$$

for the most probable exit energy E_p. We form

$$d(R_o - R_p) = \frac{dI}{I} \times (R_o q_o - R_p q_p) \tag{29},$$

noting that $R_o - R_p$ is equal to the sample thickness x to the assumed degree of approximation. R_o and R_p are obtained by numerical integration

$$R_o = \int_{2\,MeV}^{E_o} \frac{dE}{\left|\frac{dE}{ds}\right|} \tag{30}$$

$$R_p = \int_{2\,\mathrm{Mev}}^{E_p} \frac{dE}{\left|\frac{dE}{ds}\right|} \tag{31}$$

with the "best" values of I and C in the expression for $\frac{dE}{ds}$

$$R_o - R_p = \int_{E_p}^{E_o} \frac{dE}{\left|\frac{dE}{ds}\right|} \tag{32}$$

and hence

$$\frac{d(R_o - R_p)}{dE_p} = -\left|\frac{dE}{ds}\right|^{-1}_{E=E_p} \tag{33}$$

Thus,

$$\frac{dI}{I} = \frac{dE_p}{R_o q_o - R_p q_p} \times \frac{1}{-\left|\frac{dE}{ds}\right|_{E_p}} \tag{34}$$

and

$$\frac{d\ln I}{dE_p} = \frac{1}{R_o q_o - R_p q_p} \times \frac{1}{-\left|\frac{dE}{ds}\right|_{E_p}} \tag{34a}$$

The right-hand membrane of eq (34a) is composed only of known functions, and therefore, we may solve a value of $\Delta \ln I$ by inserting ΔE_p from eq. 25 for dE_p.

Our adjusted value of $\ln I$ is obtained by adding algebraically $\Delta \ln I$ to the value of $\ln I$ used in the Monte Carlo calculation.

VI. Resulting accuracies.

The standard deviations in the experimental and theoretical determinations of E_p (and E_{MC}) have been derived in sections II and IV. The Monte Carlo calculations should be carried to an accuracy such that $D^2(E_{MC}) << D^2(E_p)$. The total uncertainty in the determination of the peak energy will be

$$D_{tot} = \sqrt{D^2(E_{MC}) + D^2(E_p)} \tag{35}$$

Insertion of D_{tot} as dEp in eq. (34a) gives the resulting uncertainty in our determination of $\ln I$.

$$D(\ln I) = D_{tot} \times \left| \left[\frac{1}{R_o q_o - R_p q_p} \right] \left[\frac{1}{-\left| \frac{dE}{dS} \right|_{E_p}} \right] \right| \tag{36}$$

We pointed out in the introduction that the source energy is known only to within a certain accuracy ΔE_o. The parameters under investigation are slowly varying functions of energy (I is constant!) so that this uncertainty should not be important. If we assume, however, that the experiment was, indeed, performed at the exact source energy E_0 we should extract a corresponding deviation $\Delta \ln I$ by inserting $-\Delta E_o$ for ΔE_p in eq. (34a).

The effect of the uncertainty Δx in the assessment of the sample thickness x on ln I may be solved from eq. (29) by inserting Δx for $d(R_o - R_p)$ and solving for $d \ln I^0$.

Appendix C

The following four abstracts are of papers presented at the Sixty-eighth annual meeting of the Texas Academy of Science, December 1964.

Linear and Monte Carlo Calculations of Stopping Power and Energy Straggle

George W. Crawford
Southern Methodist University

Theoretical and Experimental Studies of energy absorption from protons in metals, plastics and biological tissues are being carried out over a range of proton energies of interest to space exploration. The theoretical study is being accomplished in three distinct steps and is based on the realization that when a charged particle traverses matter it encounters a multitude of elastic and inelastic collision processes both with orbital electrons and nuclei.

The linear transport calculations are based on the familiar Bethe-Block stopping power equation and include shell corrections. The Monte Carlo program considers the particles as moving about in non-linear paths and loosing energy continuously. A Monte Carlo nuclear interaction program is being written.

Results of the calculations are presented.

Preliminary Report of the Experimental Determination of I_{eff}, Z_{eff}, and A_{eff} in the Bethe-Bloch Stopping Power Equation for Four Plastics

James R. Cummins, Jr.
Southern Methodist University

Data is reported from which the stopping power of plastics at 36 MeV has been measured. The purpose of this study has been to help establish a proper method of applying the stopping power equation to plastics. In particular, to find a method of determining an effective mean ionization potential, an effective atomic weight and an effective charge number for each plastic. The plastics used in this study were Nylon (01, Plexiglas, and high- and low-density polyethylene.)

Stopping Power Measurements of Aℓ, Cu, and Si Using 36.1 MeV Protons

Daniel C. Nipper
Southern Methodist University

The experimental procedure for measuring linear transport stopping power is described. Data obtained using Aℓ, Cu, Si and C foils inserted in a beam of 36.1 MeV protons are presented. The Aℓ and Cu data are used as part of the calibration procedure in order to measure the mean ionization potential of metals, plastics and biological tissues.

The Preparation of Lithium-Drifted Solid State Radiation Detectors

Bobby Snow
Southern Methodist University

The theory and fabrication techniques for building lithium drifted solid state radiation detectors are discussed. Variations from existing techniques and their significance on the detection characteristics and device noise are listed and explained. Lastly, the proposed method of preparing a 1 cm x 1 cm sensitive device is outlined.

Experimental Calibration of Lithium Drifted Silicon Detectors as a Function of Proton Energy and Proton Path Length in the Detector

George W. Crawford
Southern Methodist University

The charge pulse created in Lithium drifted Silicon detectors has been measured as a function of incident energy of the proton and its path length in the sensitive volume of the detector. The nearly monoenergetic protons used were provided by the radiation facilities available at the University of Texas (8-14 Mev), the University of Southern California (18-30 Mev), Oak Ridge National Laboratories (36 Mev), and the University of Minnesota (40 Mev). The family of detectors used in the study provided path lengths in the sensitive volume as short as 100 microns and as long as 15 centimeters. Measurements were made to an accuracy of 1%. Over the energy range studied, the charge pulse created is directly proportional to the energy lost by the proton. Silicon stopping power measurements were made using both detectors and silicon absorbers.

Range-Energy and stopping power tables for Silicon have been prepared based on the experimental data. A Monte Carlo proton program has been used to calculate theoretical values for comparison with the experimental values. A mean ionization potential, I, for silicon has been obtained which permits matching of the calculated mean energy loss, peak full width half maximum, and shape of the peak with the measured value.

The above abstract is accepted for presentation at the American Physical Society meeting, 2-4 September, 1965, at Honolulu, Hawaii.

Appendix A

ANNUAL MONTE CARLO PROTON TRANSPORT PROGRAM PROGRESS REPORT

to

THE NATIONAL AERONAUTICS AND SPACE ADMINISTRATION

for

NsG 708

A GRANT IN SUPPORT

of

BASIC RESEARCH IN SEMICONDUCTOR DETECTOR-DOSIMETER CHARACTERISTICS, AS APPLIED TO THE PROBLEMS OF WHOLE BODY DOSIMETRY

from

SOUTHERN METHODIST UNIVERSITY
Dallas, Texas 75222

August, 1965

I. Introduction

The physical background of the program has been given in ref. 1, and the symbols of that reference will be retained here. The present report describes the computer program which is written in FORTRAN II language for the ~~IBM 7090~~ CDC 3400 computer. Information will be given on input data preparation and on the interpretation of the output. A sample problem will be provided.

II. Composition of the program (see flow charts in figs. 1 and 2)

II. a. Main program

The main program is labelled PROTOS. Its purpose is to call the various subroutines.

II. b. Subroutines

PDATA. This subroutine reads the physical data, i.e. source energy (E_o), cut-off energy (E_n), atomic number of the slowing-down medium (Z) etc. The tables of $(\frac{dE}{\rho dx})_i$ and straggling variance $\langle \Delta s^2 \rangle_i$ are also read. Also the tables of data needed for computing angular deviations are read by this subroutine. A table of energy points equi-distributed in the logarithm of the energy between source and cut-off energies is prepared. For each energy step three integrals are evaluated by Gaussian integration, giving values of $\langle s \rangle_i$, $\chi^2_{c,i}$ and $\log \langle \chi^2_a \rangle_i$ which are used to produce the three tables of $\langle s_i \rangle$, $\chi_{c,i}$, and B_i. A fourth table, of $\langle \Delta s^2 \rangle_i = \langle s^2 \rangle_i - \langle s \rangle^2_i$, is also prepared.

GDATA. This subroutine reads data specifying the geometry of the problem under consideration and parameters governing the output. The value of the maximum number of protons to be followed is also

direction, receiving information from subroutines ANGLE and STATI.

ANGLE. Selects the polar deviation angles and computes the quantity $\langle\omega^2\rangle$ (mean square polar deviation angle).

STATI. In this subroutine it is checked whether the proton has just passed a geometrical boundary. If so, the appropriate statistical scoring is performed.

OUT. Prepares the output when the calculation is completed.

RANDOM. Gives uniformly distributed numbers.

RNORM. Gives normally distributed numbers.

III. Description of input data

PROTOS

A time limit TMAX in minutes is read in format (F10.0).

TMAX compares with the internal clock of the computer. An integral indicator I, format (I5), controls the reading of data. It is read between the actual data sets.

I=1 calls PDATA and returns to PROTOS for a new I

I=2 " GDATA "-

I=3 " GEO "- TMAX and I

I≠1,2,3 prints out "WRONG INDICATOR" and stops the computation.

To demonstrate the use of the indicator we show the composition of the data deck for a run of three problems with two sets of physical data and three sets of geometrical data

	Read by
TMAX	PROTOS
(I=)1	PROTOS

data	GDATA
(I=)3	PROTOS (GEO) (first calculation)
TMAX	PROTOS
(I=)1	PROTOS
data	PDATA
(I=)2	PROTOS
data	GDATA
(I=)3	PROTOS (GEO) (second calculation)
TMAX	PROTOS
(I=)2	PROTOS
data	GDATA
(I=)3	PROTOS (GEO) (third calculation)
(I=)4	PROTOS (termination)

(The third problem uses the same set of PDATA as the second one).

PDATA

On the first card, a set of six data, format (2F5.0, 3I5, F5.0), is punched, viz.

EO: Source energy in MeV.

RO: Density in grams per cc.

N: Number of arguments in the table of stopping power ($N \leq 100$).

M: Number of energy points in logarithmic slowing-down scale ($M \leq 500$).

The number of energy steps is M-1.

NI: Number of arguments for table of range variance ($NI \leq 100$).

ES: Cut-off energy in MeV.

The second card contains three data, format (2F5.0, E10.3), viz.

Z: Atomic number of scattering atoms (or charge number of molecules).

(... of 1 ... fig. 1)

M the atomic (or molecular) weight.

The next cards contain a series of vectors, each vector beginning on a new card. The format is (7F10.0) throughout.

EN: N arguments (in MeV) for stopping power table ($EN_i < EN_{i+1}$).

DES: N values of the stopping power (in grams per cc) given at the arguments EN and in the same order as EN.

EE: NI arguments (in MeV) for the range variance ($EE_i < EE_{i+1}$).

EPS: NI values of the variance in sq·cm. EPS can be obtained by using the quantities ϵ_p in ref. 2, table I, applying the relation

$$(EPS)_i = \left[\frac{(\epsilon_p)_i}{100} \cdot R_i \right]^2$$

where $R_i = \int_{2\ \mathrm{MeV}}^{(EE)_i} \frac{dE}{\left|\frac{dE}{ds}\right|}$

which can be obtained for example from ref. 3, table II.

GDATA

The first card contains seven data, format (4I5, F5.0, 2I5). See figs. 3 and 4.

ND: Number of scatterer thicknesses (rod lengths) to be considered in one problem (ND≤50).

NR: Number of circles or squares to be used to define the transversal distribution of protons leaking through the end face (away from the entrance face), (NR≤20).

NT: Max. number of proton histories to be analysed. Generally, the run is terminated after a certain computing time; NT is then set to be a large number, say, 50000.

R: Radius of source in cm.

KU: Conversion factor from internal energy scale (determined by M) to output energy scale. This is discussed further below (chapt. V).

IG: Constant which determines whether the scatterer is to be bounded by a surface (parallel to the direction of the entering protons) with circular or square cross-section. IG=0 in the circular case and IG=1 in the square case.

The following 3 sets of vectors are read in format (7F10.0), each vector starting on a new card. See figs. 3 and 4.

RU: NR values of circle radii or half square sides ($RU_i < RU_{i+1}$) for definition of transversal distributions (in cm). Max (RU) defines the external surface.

DU: ND values of scatterer thickness (rod length) in cm.

THET: NTH values of cos for definition of angular distribution histogram $THET_i < THET_{i+1}$. The last value must be equal to 1.0.

Due to storage restrictions the following criterion has to be fulfilled in addition to those stated above: $ND \times NR \times NTH \times \left[\frac{M-1}{KU} - 1\right] \leq 5000$.

IV. Description of output

The output starts by reproducing the physical data. The succeeding three columns, labelled EK, DS, and PRO contain 1) the M energy values for the slowing down formalism (denoted E_i in ref. 1), 2) M corresponding values of $\langle s_i \rangle$ (see ref. 1, page 8), and 3) M values of $(\langle \Delta s^2 \rangle_i)^{\frac{1}{2}}$ (see ref. 1, page 8). Then the remainder of the input data is reproduced.

The Monte Carlo results are given separately for each scatterer thickness (rod length), indicated by the z coordinate. All results are given in protons per MeV and are normalized to one source proton. This

by its standard deviation as an indication of the probable error. The text which is printed in the output is sufficient for orientation. The last set of results is the energy distribution of protons leaking out through the lateral sides of the longest scatterer.

V. A note on energy scales

The internal energy scale is defined through the values of EO, ES, and M, given in the input. The resulting energy points will be EO, $k\cdot(EO)$, $k^2\cdot(EO)$,.....$k^{M-1}(EO) = ES$. k is the quantity used in ref. 1 and is obtained by the relation $\ln k = [\ln(ES/EO)]:(M-1)$. As discussed in ref. 1, the boundaries of the energy bins, upon which we base the energy distribution histogram, should coincide with points in the internal mesh. The input parameter KU determines the selection of energy points in such a way that (M-1):KU energy bins, equally spaced in the logarith of energy, will produce the histogram. If the quantity (M-1):KU is not an integral number the program will automatically adjust the upper limit of the lowest energy bin with the effect that all the energy bins except the lowest one will still have a uniform logarithmic spacing with endpoints coinciding with the internal scale.

VI. A test problem

In Appendix I we reproduce the data sheets for a test problem, in which the slowing down of protons in silicon from 187 MeV to 147 MeV is studied. The data are composed in a way to provide an allustrative problem rather than a scientifically meaningful one. The output of a run of the test problem (6 minutes on the IBM 7090) is also shown (appendix II).

References:

1. C. Johansson & M. Leimdörfer: "A Monte Carlo procedure for calculating the migration of protons taking account only of electromagnetic interactions". FOA 4 report A 4411-411, Jan 1965.

2. R.M. Sternheimer: "Range straggling of charged particles in Be, C, Al, Cu, Pb, and Air". Phys. Rev. 117 (1960) 485.

3. R.M. Sternheimer: "Range-energy relations for protons in Be, C, Al, Cu, Pb, and Air". Phys. Rev. 115 (1960) 137.

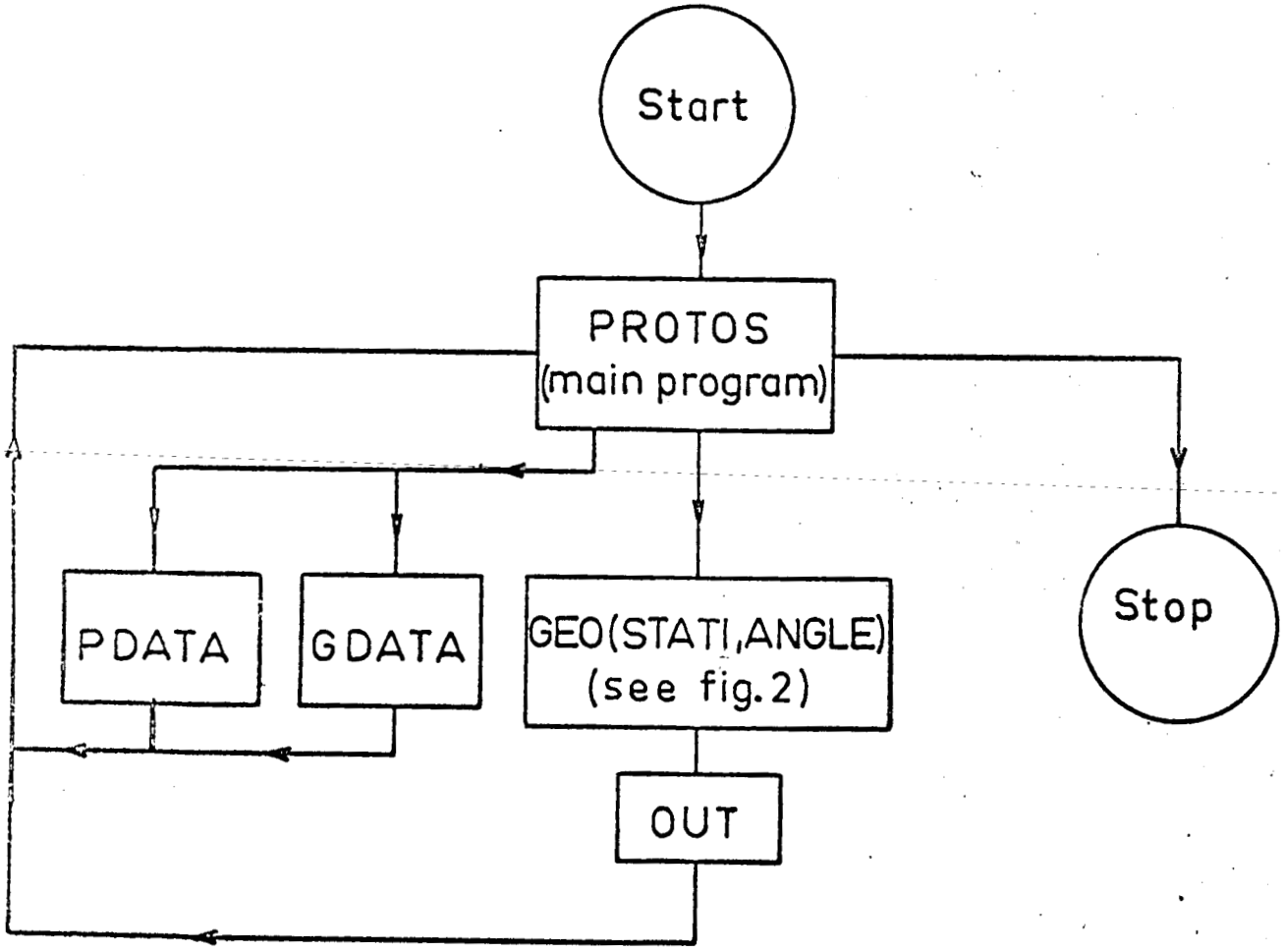

Fig.1. Flow scneme showing principal program structure

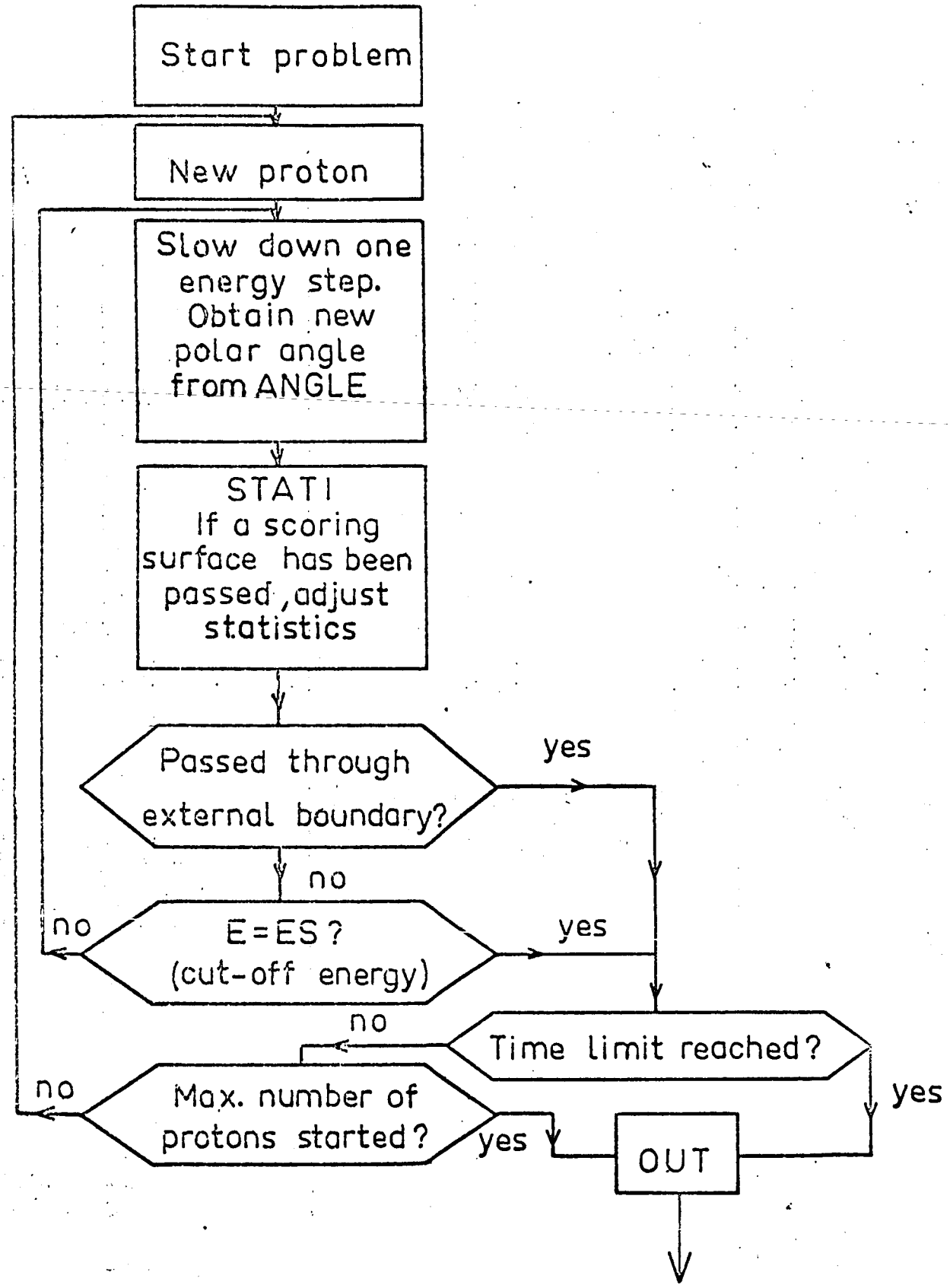
Start problem
New proton
Slow down one energy step. Obtain new polar angle from ANGLE
STATI
If a scoring surface has been passed, adjust statistics
Passed through external boundary?
yes
no
E=ES?
(cut-off energy)
no
yes
Time limit reached?
no
yes
Max. number of protons started?
no
yes
OUT

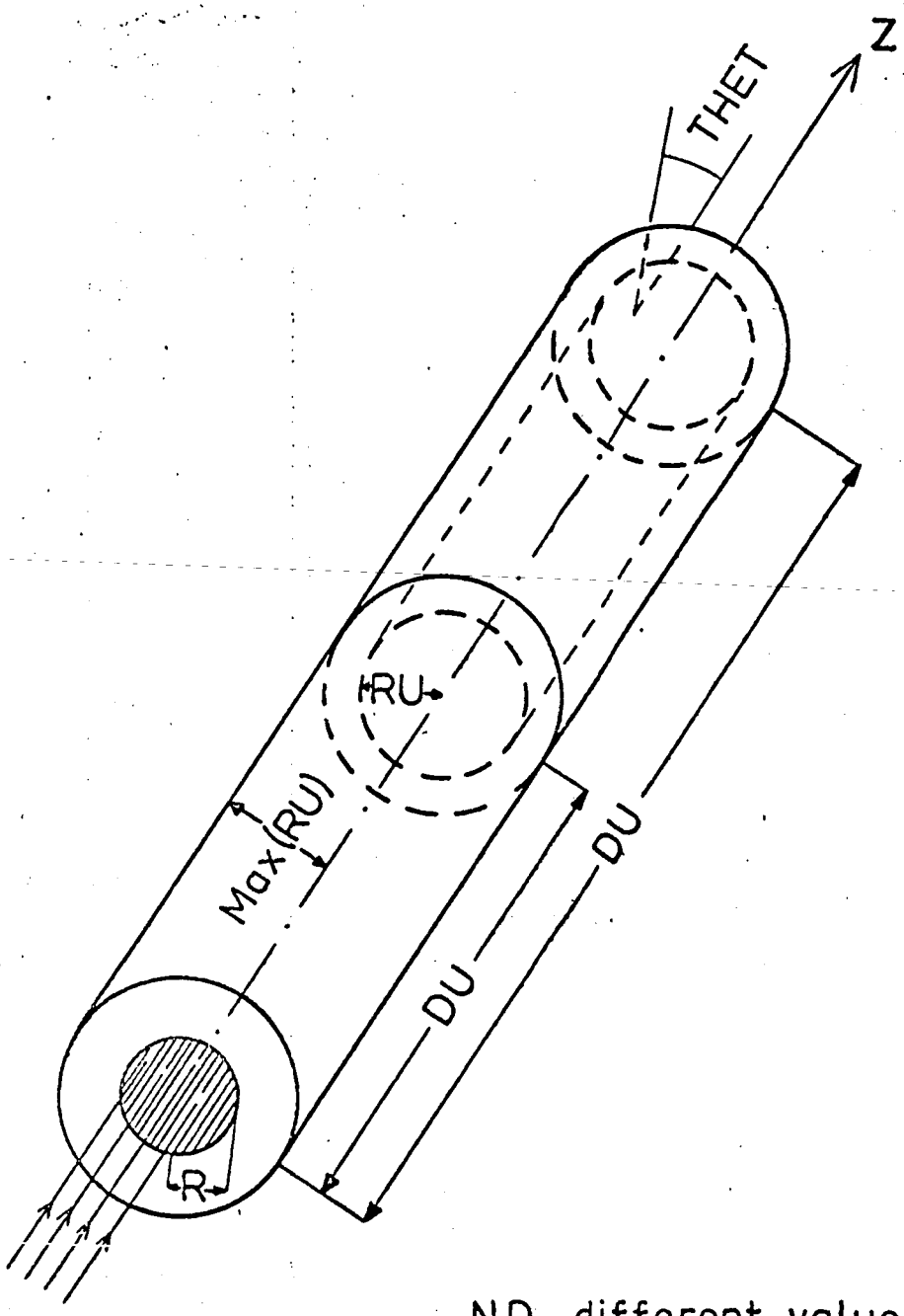

Source protons

ND different values of DU
NR different values of RU
NTH different values of THET

Fig.2 Sketch of circular end geometry (IGC=2)

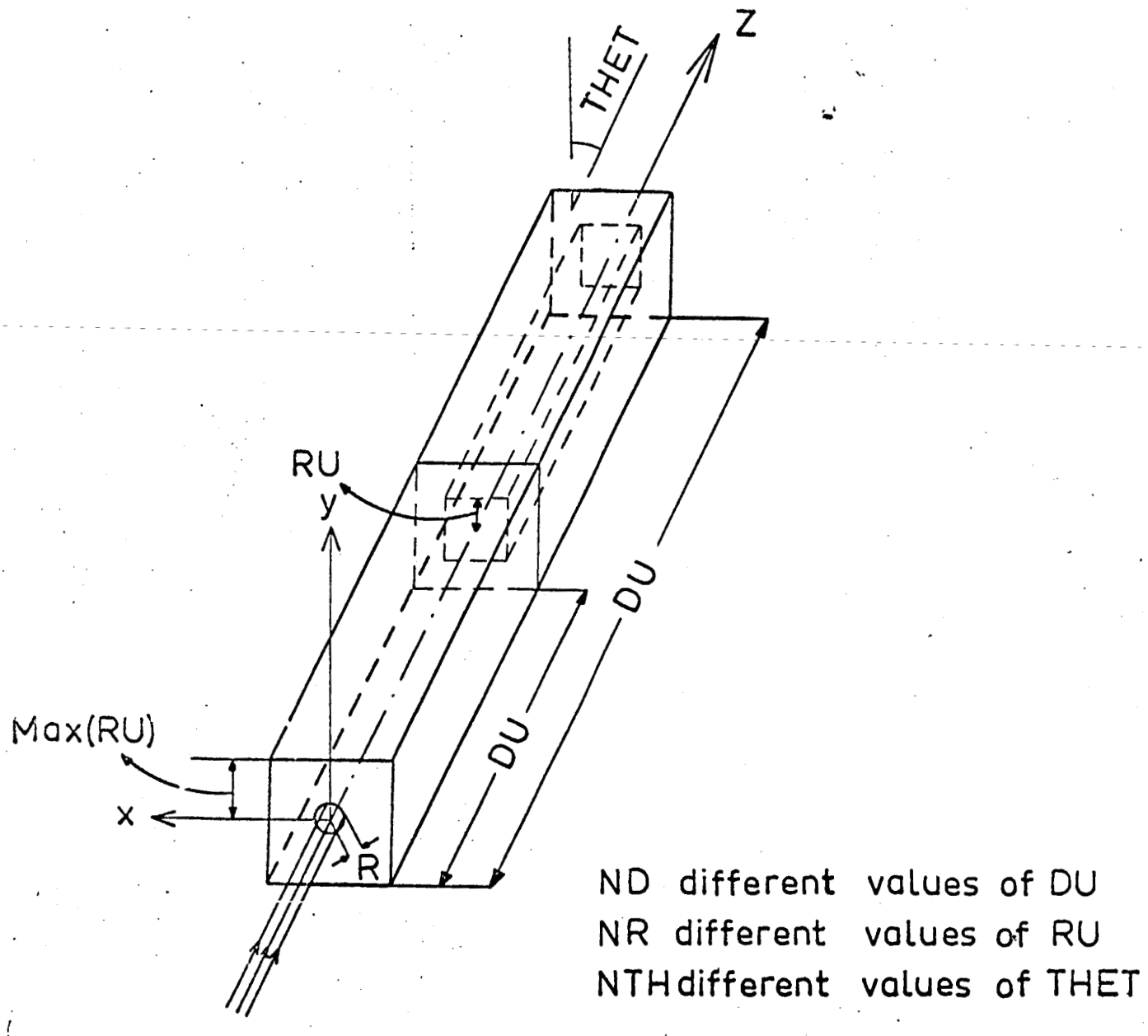

Fig.4. Sketch of square rod geometry (IG=1)

DATA

Programmets namn: /

Tfn: | Datum: | Signatur: | Page 1 | Antal blad:

1–10	11–20	21–30	31–40	41–50	51–60	61–72	73–80 READ BY
							PROTOS
							PROTOS
33	38 50	20 147					PDATA
.2	.4996E23						-"-
2	3	4	5	6	7	8	-"-
9	10	12	14	16	18	20	-"-
.5	25	27.5	30	35	40	45	-"-
50	55	60	65	70	75	80	-"-
90	100	110	120	130	140	150	-"-
60	180	200	225	250	275	300	-"-
28	86.38468	71.56402	60.55046	52.72335	46.84633	42.25555	-"-
91	35.51730	30.78478	27.26274	24.24418	22.11890	20.37010	-"-
60	17.0988	15.8548	14.8172	13.1304	11.8306	10.7924	-"-
54	9.2240	8.6229	8.1063	7.6557	7.2866	6.9402	-"-
52	5.8829	5.4716	5.1608	4.8772	4.6318	4.4175	-"-
87	3.9114	3.6584					-"-
2	4	6	8	10	15	20	-"-
25	30	40	50	60	70	80	-"-
00	120	140	160	200	250		-"-
.8	7.292E-8	.2578E-6	.6379E-6	1.297E-6	4.800E-6	.1219E-4	-"-
-4	.4636E-4	1.203E-4	2.538E-4	4.663E-4	7.783E-4	.1214E-2	-"-
-2	.4640E-2	.7660E-2	1.182E-2	2.417E-2	4.684E-2		-"-

DATA

Programmets namn | Tfn | Datum | Signatur | Page XXXXXX 2 | Antal blad

```
10  11        20  21        30  31        40  41        50  51        60  61        72  73        80
                                                                                    PROTOS
3100000     2.564     50                                                            GDATA
5       1.0     1.5                                                                   -"-
5   2.170   3.193   4.174                                                             -"-
5       1.0                                                                       -"-
                                                                                    PROTOS
                                                                                      -"-
```


l à 100 ex

NEW PHYSICAL DATA

=187.0 RO= 2.33 NUMBER OF STEPS= 50 Z= 14. CE=-5.20 E OUT OFF=147.0

ERGY SCALE FOR STOPPING POWER

.2000E 01	0.3000E 01	0.4000E 01	0.5000E 01	0.6000E 01	0.7000E 01	0.8000E 01
.9000E 01	0.1000E 02	0.1200E 02	0.1400E 02	0.1600E 02	0.1800E 02	0.2000E 02
.2250E 02	0.2500E 02	0.2750E 02	0.3000E 02	0.3500E 02	0.4000E 02	0.4500E 02
.5000E 02	0.5500E 02	0.6000E 02	0.6500E 02	0.7000E 02	0.7500E 02	0.8000E 02
.9000E 02	0.1000E 03	0.1100E 03	0.1200E 03	0.1300E 03	0.1400E 03	0.1500E 03
.1600E 03	0.1800E 03	0.2000E 03				

)PPING POWER

.1007E 03	0.8838E 02	0.7156E 02	0.6055E 02	0.5272E 02	0.4685E 02	0.4226E 02
.3856E 02	0.3552E 02	0.3078E 02	0.2726E 02	0.2424E 02	0.2212E 02	0.2037E 02
.1857E 02	0.1710E 02	0.1586E 02	0.1482E 02	0.1313E 02	0.1183E 02	0.1079E 02
.9935E 01	0.9224E 01	0.8623E 01	0.8106E 01	0.7656E 01	0.7287E 01	0.6940E 01
.6355E 01	0.5883E 01	0.5472E 01	0.5161E 01	0.4877E 01	0.4632E 01	0.4417E 01
.4229E 01	0.3911E 01	0.3658E 01				

:RGY SCALE FOR VARIANCE

2000E 01	0.4000E 01	0.6000E 01	0.8000E 01	0.1000E 02	0.1500E 02	0.2000E 02
2500E 02	0.3000E 02	0.4000E 02	0.5000E 02	0.6000E 02	0.7000E 02	0.8000E 02
1000E 03	0.1200E 03	0.1400E 03	0.1600E 03	0.2000E 03	0.2500E 03	

IANCE

9007E-08	0.7292E-07	0.2578E-06	0.6379E-06	0.1297E-05	0.4800E-05	0.1219E-04
2535E-04	0.4636E-04	0.1203E-03	0.2538E-03	0.4663E-03	0.7783E-03	0.1214E-02
2541E-02	0.4640E-02	0.7660E-02	0.1182E-01	0.2417E-01	0.4884E-01	

EK	DS	PRO
0.1870E 03	0.	0.
0.1861E 03	0.1029E-00	0.1754E-01
0.1852E 03	0.1021E-00	0.1739E-01
0.1843E 03	0.1012E-00	0.1725E-01
0.1834E 03	0.1004E-00	0.1711E-01
0.1825E 03	0.9961E-01	0.1697E-01
0.1816E 03	0.9881E-01	0.1684E-01
0.1807E 03	0.9801E-01	0.1670E-01
0.1798E 03	0.9722E-01	0.1656E-01
0.1789E 03	0.9644E-01	0.1642E-01
0.1780E 03	0.9566E-01	0.1628E-01
0.1772E 03	0.9489E-01	0.1615E-01
0.1763E 03	0.9412E-01	0.1601E-01
0.1754E 03	0.9336E-01	0.1588E-01
0.1746E 03	0.9260E-01	0.1574E-01
0.1737E 03	0.9185E-01	0.1561E-01
0.1729E 03	0.9111E-01	0.1547E-01
0.1720E 03	0.9037E-01	0.1534E-01
0.1712E 03	0.8963E-01	0.1520E-01
0.1703E 03	0.8891E-01	0.1507E-01
0.1695E 03	0.8818E-01	0.1494E-01
0.1687E 03	0.8747E-01	0.1481E-01
0.1678E 03	0.8675E-01	0.1467E-01
0.1670E 03	0.8605E-01	0.1454E-01
0.1662E 03	0.8535E-01	0.1441E-01
0.1654E 03	0.8465E-01	0.1428E-01
0.1646E 03	0.8396E-01	0.1415E-01
0.1638E 03	0.8327E-01	0.1402E-01
0.1630E 03	0.8259E-01	0.1389E-01
0.1622E 03	0.8192E-01	0.1376E-01
0.1614E 03	0.8125E-01	0.1364E-01
0.1606E 03	0.8058E-01	0.1351E-01
0.1598E 03	0.7992E-01	0.1349E-01
0.1590E 03	0.7927E-01	0.1370E-01
0.1582E 03	0.7862E-01	0.1359E-01
0.1575E 03	0.7798E-01	0.1348E-01
0.1567E 03	0.7734E-01	0.1337E-01
0.1559E 03	0.7671E-01	0.1326E-01
0.1552E 03	0.7608E-01	0.1316E-01
0.1544E 03	0.7545E-01	0.1305E-01
0.1536E 03	0.7483E-01	0.1295E-01
0.1529E 03	0.7422E-01	0.1284E-01
0.1521E 03	0.7361E-01	0.1273E-01
0.1514E 03	0.7300E-01	0.1263E-01
0.1507E 03	0.7241E-01	0.1252E-01
0.1499E 03	0.7181E-01	0.1242E-01
0.1492E 03	0.7122E-01	0.1232E-01
0.1485E 03	0.7063E-01	0.1221E-01
0.1477E 03	0.7005E-01	0.1211E-01
0.1470E 03	0.6947E-01	0.1201E-01

NEW GEOMETRICAL DATA ↓NT ↓R ↓XU ↓IC

X NUMBER OF PROTONS= 10000 SOURCE RADIUS= 0.564 OUTPUT FACTOR= 5 GEOMETRY= 0 (circular rod)

RADII

0.50 1.00 1.50

RU

LENGTHS DU

1.10 2.17 3.19 4.17

ENERGY DIVISIONS IN OUTPUT

$EO, EO \times (\frac{ES}{EO})^{\frac{KU}{M-1}}, EO \times (\frac{ES}{EO})^{\frac{2KU}{M-1}} \ldots EO \times (\frac{ES}{EO})^{\frac{M-2}{M-1} \times KU}$

0 187.0 182.5 178.0 173.7 169.5 165.4 161.4
157.5 153.6 149.9

ANGLE DIVISIONS $EO \times (\frac{ES}{EO})^{\frac{M-2}{M-1}} \times KU$

0.9995 1.0000

IME INTERRUPT NT= 351 TIME= 6.0

1.10 CM (FIRST ROD LENGTH)

187.00• E • 182.46 MEV HIGHEST ENERGY INTERVAL

0.50 CM
0. 0.
0. 0. PARTICLES ESCAPING THROUGH INNERMOST RADIAL INTERVAL ($r < 0.5$)

1.00 CM
0. 0.
0. 0. PARTICLES ESCAPING THROUGH RADIAL INTERVAL $0.5 < r < 1.0$

1.50 CM
0. 0.
0. 0. PARTICLES ESCAPING THROUGH RADIAL INTERVAL $1.0 < r < 1.5$

182.46• E • 178.04 MEV

0.50 CM
0. 0.386E-02
0. 0.156E-02

1.00 CM
0. 0.
0. 0.

1.50 CM
0. 0.
0. 0.

NO. OF PROTONS PER MEV AND STARTED PROTON $0 < \cos\theta < 0.9995$

STANDARD DEV. OF ABOVE QUANTITY

AS ON THE LEFT BUT FOR $0.9995 < \cos\theta < 1.0$

178.04• E • 173.72 MEV

0.50 CM
0. 0.184E-00
0. 0.499E-02

1.00 CM
0. 0.435E-01
0. 0.483E-02

1.50 CM
0. 0.
0. 0.

173.72• E • 169.50 MEV

```
X=       0.50  CM
  0.             0.
  0.             0.

X*       1.00  CM
  0.             0.
  0.             0.

X*       1.50  CM
  0.             0.
  0.             0.

    169.50* E *     165.39  NEV

X*       0.50  CM
  0.             0.
  0.             0.

X*       1.00  CM
  0.             0.
  0.             0.

X*       1.50  CM
  0.             0.
  0.             0.

    165.39* E *     161.38  NEV

X*       0.50  CM
  0.             0.
  0.             0.

X*       1.00  CM
  0.             0.
  0.             0.

X*       1.50  CM
  0.             0.
  0.             0.

    161.38* E *     157.46  MEV

X*       0.50  CM
  0.             0.
  0.             0.

X*       1.00  CM
  0.             0.
  0.             0.

X*       1.50  CM
  0              0.
  0.             0.

    157.46* E *     153.64  MEV

X*       0.50  CM
  0.             0.
  0.             0.
```

0. 0.

X* 1.50 CM
0. 0.
0. 0.

153.64* E * 149.92 MEV

X* 0.50 CM
0. 0.
0. 0.

X* 1.00 CM
0. 0.
0. 0.

X* 1.50 CM
0. 0.
0. 0.

149.92* E * 147.00 MEV

X* 0.50 CM
0. 0.
0. 0.

X* 1.00 CM
0. 0.
0. 0.

X* 1.50 CM
0. 0.
0. 0.

Z= 2.17 CM

187.00* E * 182.46 MEV

X* 0.50 CM
0. 0.
0. 0.

X* 1.00 CM
0. 0.
0. 0.

X* 1.50 CM
0. 0.
0. 0.

182.46* E * 178.04 MEV

X* 0.50 CM
0. 0.
0. 0.

X* 1.00 CM
0. 0.
0. 0.

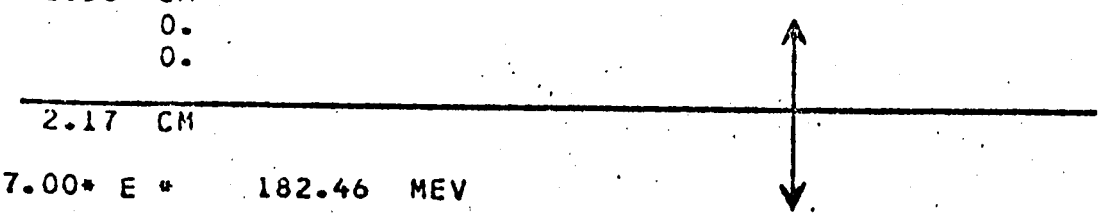

0. 0.

178.04* E * 173.72 MEV

X* 0.50 CM
0. 0.
0. 0.

X* 1.00 CM
0. 0.
0. 0.

X* 1.50 CM
0. 0.
0. 0.

173.72* E * 169.50 MEV

X* 0.50 CM
0. 0.
0. 0.

X* 1.00 CM
0. 0.
0. 0.

X* 1.50 CM
0. 0.
0. 0.

169.50* E * 165.39 MEV

X* 0.50 CM
0.970E-02 0.186E-00
0.254E-02 0.549E-02

X* 1.00 CM
0.208E-02 0.443E-01
0.119E-02 0.501E-02

X* 1.50 CM
0. 0.
0. 0.

165.39* E * 161.38 MEV

X* 0.50 CM
0. 0.
0. 0.

X* 1.00 CM
0. 0.710E-03
0. 0.709E-03

X* 1.50 CM
0. 0.
0. 0.

```
  0.          0.

X*      1.00  CM
  0.          0.
  0.          0.

X*      1.50  CM
  0.          0.
  0.          0.

    157.46* E *    153.64  MEV

X*      0.50  CM
  0.          0.
  0.          0.

X*      1.00  CM
  0.          0.
  0.          0.

X*      1.50  CM
  0.          0.
  0.          0.

    153.64* E *    149.92  MEV

X*      0.50  CM
  0.          0.
  0.          0.

X*      1.00  CM
  0.          0.
  0.          0.

X*      1.50  CM
  0.          0.
  0.          0.

    149.92* E *    147.00  MEV

X*      0.50  CM
  0.          0.
  0.          0.

X*      1.00  CM
  0.          0.
  0.          0.

X*      1.50  CM
  0.          0.
  0.          0.

Z=      3.19  CM

    187.00* E *    182.46  MEV

X*      0.50  CM
  0.          0.
  0.          0.
```

0. 0.

X* 1.50 CM
0. 0.
0. 0.

182.46* E * 178.04 MEV

X* 0.50 CM
0. 0.
0. 0.

X* 1.00 CM
0. 0.
0. 0.

X* 1.50 CM
0. 0.
0. 0.

178.04* E * 173.72 MEV

X* 0.50 CM
0. 0.
0. 0.

X* 1.00 CM
0. 0.
0. 0.

X* 1.50 CM
0. 0.
0. 0.

173.72* E * 169.50 MEV

X* 0.50 CM
0. 0.
0. 0.

X* 1.00 CM
0. 0.
0. 0.

X* 1.50 CM
0. 0.
0. 0.

169.50* E * 165.39 MEV

X* 0.50 CM
0. 0.
0. 0.

X* 1.00 CM
0. 0.

165.39* E * 161.38 MEV

X* 0.50 CM
0. 0.
0. 0.

X* 1.00 CM
0. 0.
0. 0.

X* 1.50 CM
0. 0.
0. 0.

161.38* E * 157.46 MEV

X* 0.50 CM
0.946E-02 0.524E-01
0.257E-02 0.551E-02

X* 1.00 CM
0.728E-03 0.160E-01
0.727E-03 0.330E-02

X* 1.50 CM
0. 0.
0. 0.

157.46* E * 153.64 MEV

X* 0.50 CM
0.172E-01 0.133E-00
0.346E-02 0.698E-02

X* 1.00 CM
0.149E-02 0.291E-01
0.105E-02 0.439E-02

X* 1.50 CM
0. 0.
0. 0.

153.64* E * 149.92 MEV

X* 0.50 CM
0. 0.
0. 0.

X* 1.00 CM
0. 0.
0. 0.

X* 1.50 CM
0. 0.
0. 0.

149.92* E * 147.99 MEV

X* 1.00 CM
0. 0.
0. 0.

X* 1.50 CM
0. 0.
0. 0.

Z= 4.17 CM

187.00* E * 182.46 MEV

X* 0.50 CM
0. 0.
0. 0.

X* 1.00 CM
0. 0.
0. 0.

X* 1.50 CM
0. 0.
0. 0.

182.46* E • 178.04 MEV

X* 0.50 CM
0. 0.
0. 0.

X* 1.00 CM
0. 0.
0. 0.

X* 1.50 CM
0. 0.
0. 0.

178.04* E * 173.72 MEV

X* 0.50 CM
0. 0.
0. 0.

X* 1.00 CM
0. 0.
0. 0.

X* 1.50 CM
0. 0.
0. 0.

173.72* E • 169.50 MEV

X* 0.50 CM
0. 0.
0 0.

X* 1.50 CM
0. 0.
0. 0.

169.50* E * 165.39 MEV

X* 0.50 CM
0. 0.
0. 0.

X* 1.00 CM
0. 0.
0. 0.

X* 1.50 CM
0. 0.
0. 0.

165.39* E * 161.38 MEV

X* 0.50 CM
0. 0.
0. 0.

X* 1.00 CM
0. 0.
0. 0.

X* 1.50 CM
0. 0.
0. 0.

161.38* E * 157.46 MEV

X* 0.50 CM
0. 0.
0. 0.

X* 1.00 CM
0. 0.
0. 0.

X* 1.50 CM
0. 0.
0. 0.

157.46* E * 153.64 MEV

X* 0.50 CM
0. 0.
0. 0.

X* 1.00 CM
0. 0.
0. 0.

```
X*        0.50   CM
  0.                0.
  0.                0.

X*        1.00   CM
  0.                0.
  0.                0.

X*        1.50   CM
  0.                0.
  0.                0.

    149.92* E =     147.00   MEV

X*        0.50   CM
  0.254E-01         0.957E-01
  0.479E-02         0.821E-02

X*        1.00   CM
  0.488E-02         0.303E-01
  0.217E-02         0.519E-02

X*        1.50   CM
  0.                0.
  0.                0.
```

187.00* E * 182.46 MEV
0. 0.

182.46* E * 178.04 MEV
0. 0.

178.04* E * 173.72 MEV
0. 0.

173.72* E * 169.50 MEV
0. 0.

169.50* E * 165.39 MEV
0. 0.

165.39* E * 161.38, MEV
0. 0.

161.38* E * 157.46 MEV
0.

157.46* E * 153.64 MEV
0.

153.64* E * 149.92 MEV
0. 0.

149.92* E * 147.00 MEV
0. 0.

STAND. DEV. OF QUANTITY ON THE LEFT

NO. OF PROTONS ESCAPING THROUGH LATERAL SURFACE PER MEV IN ENERGY INTERVAL 187 < E < 182.46 MEV PER STARTED PROTON (ROD LENGTH 4.17 CM)